Journal of Occupational and Environmental Hygiene, 4: 363–374
ISSN: 1545-9624 print / 1545-9632 online
DOI: 10.1080/15459620701277468

Estimating Service Lives of Organic Vapor Cartridges III: Multiple Vapors at All Humidities

Gerry O. Wood[1] and Jay L. Snyder[2]

[1]Consultant, Los Alamos, New Mexico
[2]National Personal Protective Technology Laboratory, NIOSH/CDC/DHHS, Pittsburgh, Pennsylvania

A published model for estimating service lives of organic vapor (OV) air-purifying respirator cartridges has been extended to include multiple organic vapors at all humidities. Equilibria among the OVs are calculated using Ideal Adsorbed Solution Theory, whereas the effects of adsorbed water are considered as due to micropore volume exclusion. Solubilities of OVs in water must also be taken into account. Adsorption kinetics of components of mixtures are based on published correlations of the effects of covapors and water vapor. The dynamics of adsorption and competition are incorporated using expanding zones within the carbon bed, taking into account vapor and water displacements. Measurements of breakthrough curves for two ternary OV mixtures at high humidities have been done for a single cartridge type. The service life estimation model, implemented as a spreadsheet and a computer program, has been tested against these data as well as data for OV mixtures from literature sources. Good agreements were obtained between model predictions and experimental breakthrough times at dry conditions and humid conditions.

Keywords cartridge, mixtures, organic vapor, respirator, service life

Address correspondence to: Gerry O. Wood, 40 San Juan Street, Los Alamos, NM 87544; e-mail: GerryConsulting@cs.com.

INTRODUCTION

In the absence of end-of-service life indicators for organic vapor (OV), air-purifying respirator cartridges, measurements, and/or predictive models must be relied on to set required change-out schedules.[1] Previous reports have presented models for estimating service lives of OV cartridges for single organic vapors[2] and of other cartridges for reactive gases,[3] both at all humidities. Since there are mixtures of OVs present in some workplaces, there is still a need to take into account the competitive interactions of multiple vapors with each other and with water.

Several researchers have measured breakthrough times or breakthrough curves for mixtures (usually binary and dry) of OVs with respirator cartridges. However, most of these studies were performed with binary mixtures at dry conditions. Additional data for multivapor mixtures at high humidities are needed to develop and test service life predictive models.

The scope of the work presented here is to extend the previous equation-based, single-vapor model to handle mixtures of vapors at all humidities. Published data for OV mixtures and cartridges were identified for testing this model. New breakthrough time data for OV mixtures at high humidities were developed for comparisons with model predictions. The practical goal of the model presented here is to be able to predict when cartridges no longer provide a worker with adequate protection. Estimations of breakthrough times for each vapor component at selected acceptable breakthrough limits can be applied to estimate service lives and (perhaps with a safety factor) set change-out schedules.

BACKGROUND

In 1998 the Occupational Safety and Health Administration published two rules of thumb based on the best information available at the time:

> Where the individual compounds in the mixture have similar breakthrough times (i.e., within one order of magnitude), service life of the cartridge should be established assuming the mixture stream behaves as a pure system of the most rapidly migrating component or compound with the shortest breakthrough time (i.e., sum up the concentration of the components). Where the individual compounds in the mixture vary by two orders of magnitude or greater, the service life may be based on the contaminant with the shortest breakthrough time.[4]
>
> Predictions based upon models without experimental data should probably be very conservative and ascribe the service life derived from the least well adsorbed compound to the total mixture concentration in terms of parts per million. The displacement of a less well adsorbed compound by a more highly adsorbed one may alter the actual service life from the estimated one in some cases.[5]

These guidelines reflect the expected phenomena of competition and displacement but are confusing to understand and apply and may be overly conservative.

Equation-based models for estimating service lives of OV cartridges have been published for single vapors at dry and all-humidity conditions.[2,6] They are based on the Reaction Kinetic form of the Wheeler-Jonas equation:[7]

$$t_b = \frac{W_e W}{C_o Q} - \frac{W_e \rho_B}{k_v C_o} \ln\left(\frac{C_o - C}{C}\right) \quad \textbf{(1)}$$

which includes (1) carbon bed parameters of bed weight W (g) and packed density ρ_B (g/cm^3); (2) use parameters of challenge vapor concentration C_o (g/cm^3), breakthrough concentration C (g/cm^3), and airflow rate Q (cm^3/min); and (3) vapor/carbon interaction parameters of adsorption rate coefficient k_v (min^{-1}) and adsorption capacity W_e (g/g carbon) at C_o. With these units, breakthrough time t_b is in minutes. A computer application has been distributed for the single-vapor, all-humidity model.[8]

These models also rely on the Dubinin-Radushkevich (DR) equation to calculate equilibrium adsorption capacity W_e (g/g carbon) of individual organic vapors:[9]

$$W_e = W_o d_L \exp[-(RT/\beta E_o)^2 \{\ln(p_{sat}/p)\}^2] \quad \textbf{(2)}$$

where W_o (cm^3/g) is the micropore volume of the carbon and E_o (kJ/mol) is its reference adsorption energy; d_L (g/cm^3) is the liquid density of the adsorbate; p_{sat} is the vapor pressure of its unadsorbed bulk (liquid) form at temperature T (°K); and β is its relative affinity coefficient (no units).

At high humidities, such capacities are reduced by micropore volume exclusion by adsorbed water, whereas an opposite effect is to increase capacities by solubility (if any) in this water.[2] The single-vapor model used published correlations of adsorption rates of both OVs and water, an expanding zone concept with water vapor rollup due to displacement by OVs, and other effects of water and OVs on adsorption rates and capacities.[2]

Two reviews of equilibrium adsorption of binary mixtures identified the best equations for estimating capacities.[10,11] Twelve adsorption isotherm equations proposed for describing multicomponent adsorption were tested with two sets of binary mixture data.[10] Of these, the Grant-Manes (Polanyi Adsorption Theory)[12] and the Myers-Prausnitz (Ideal Adsorbed Solution Theory, IAST)[13] were the most successful, especially when combined with the DR equation.[2] Studies with additional mixture data confirmed the usefulness of the IAST/DR approach supplemented with Bering or Lewis equations.[11]

A study of the effects of OV covapors on adsorption rates produced average correction factors based on the order of elution from carbon beds.[14] Adsorption rate coefficients for first eluting vapors in mixtures were statistically no different than those of single vapors. Correction factors (rate coefficient multipliers for components of a mixture) for second eluting vapors averaged 0.85 and those for third and fourth eluting vapors averaged 0.56.

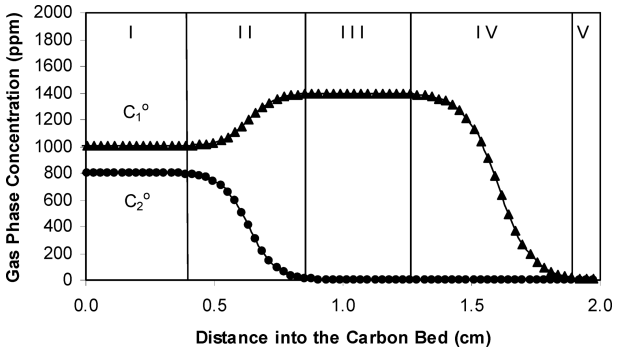

FIGURE 1. Cooney-Strusi[15] zones of vapor concentrations C_1^o and C_2^o within a 2-cm deep carbon bed challenged with a hypothetical mixture of two vapors. In Zone I, the carbon is equilibrium saturated with both vapors. In Zone II, Vapor 2 is adsorbing and displacing Vapor 1 from its saturated equilibrium. In Zone III, Vapor 1 is at equilibrium at a higher (rollup) concentration than that entering the bed. In Zone IV, Vapor 1 is adsorbing from this higher concentration without interference from Vapor 2.

Cooney and Strusi[15] defined five zones of vapor concentration within a sorbent bed with a flowing binary mixture, as shown with synthetic data in Figure 1. Complete breakthrough curves for two components can also be defined by five time zones, since such curves are obtained from vapor concentration measurements at the bed exit as the adsorption pattern moves through the bed. These corresponding breakthrough curve zones are shown in Figure 2. The rollup effect ($C_1 > C_1^o$) due to displacement of vapor 1 by vapor 2 is seen in Zones II, III, and IV.

Yoon and Lara et al.[16–19] produced a series of papers in which they show how to describe such multicomponent breakthrough curves for respirator cartridges. They fit:

$$\left(\frac{C}{C_o}\right)_i = [1 + \exp(k_i'(\tau_i - t))]^{-1} \quad \textbf{(3)}$$

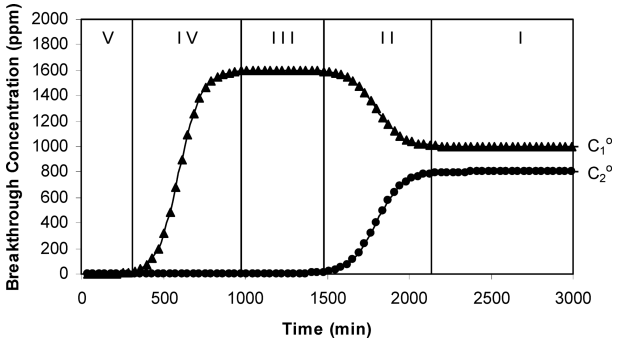

FIGURE 2. Cooney-Strusi[15] zones of vapor concentrations in bed effluent (breakthrough curves) and an example of vapor rollup from a carbon bed challenged with a hypothetical mixture of two vapors at concentrations C_1^o and C_2^o. Zones are defined as in Fig. 1.

to their experimental multicomponent breakthrough curves of each vapor i in a mixture to extract empirical constants k_i' and breakthrough curve midpoints τ_i for challenge concentrations C_{oi} and breakthrough concentrations C_i. The mixtures included acetone/m-xylene, acetone/cyclohexane/toluene, ethyl acetate/cyclohexane/toluene, cyclohexane/toluene/m-xylene, ethyl acetate/cyclohexane/toluene/m-xylene, and acetone/cyclohexane/toluene/m-xylene.

Displacement ratios and displacement fractions were also calculated from observed concentration rollups. With only a few parameters, this model was able to describe the breakthrough curves; however, these parameters were calculated from the same breakthrough curves. Therefore, this was a descriptive model instead of a predictive one.

A predictive multicomponent model would need to develop values for these parameters from independent sources, e.g., single and multiple component adsorption isotherms and rate coefficient models. Vahdat et al.[20] have taken just such an approach to transform the Yoon/Lara model[16–19] into a predictive model. They used Langmuir isotherms extracted from single-component breakthrough curves to obtain parameters to apply the IAST mixture model. Rate coefficients were obtained from single-component breakthrough times at 0.001 and 0.999 breakthrough fractions, which assumes symmetric breakthrough curves and the Wheeler/Reaction Kinetic (Eq. 1) model. This approach still lacks the ability to predict the single vapor adsorption capacity and rate parameters needed in a predictive model.

New Model Description

Expanding Zone Model

The model presented here is based on a concept of zones within the carbon bed first introduced in the single-vapor, all-humidity model.[2] These expanding zones are defined differently from those of Cooney and Strusi,[15] having zone boundaries at the centers of the mixture component wavefronts and breakthrough curves. This allows handling vapor capacities and adsorption kinetics separately. Figures 3 and 4 show the new zone definitions.

Figures 5 and 6 show a hypothetical example of the expanding zone model for five vapors. Initially, the kinetics are ignored and the component wavefronts are taken to be flat. At the beginning of cartridge or carbon bed exposure, all zones but Zone 6 have zero width (depth into the carbon bed). With time of exposure to vapors, they expand at differing rates to different widths (not the same widths as shown in the figures). The boundaries are where one of the vapors in succession is completely adsorbed and does not pass into the next zone.

For this example, five vapors at 500 ppm each are flowing into Zone 1 and maintained at these concentrations in the gas phase (Figure 5). (Note that the order in the legend is the stack order in the figures.) In the carbon phase (Figure 6), however, much more of the heptane with the highest adsorption affinity is adsorbed and much less of the methanol is retained. At some distance into the bed all the heptane is removed and only the other four vapors pass into Zone 2. This process continues until no OVs are left to pass into Zone 6. Zone 1 width increases with time as more vapors enter. Other zones expand similarly until they each in turn reach the end of the bed and an equilibrium breakthrough of each vapor occurs.

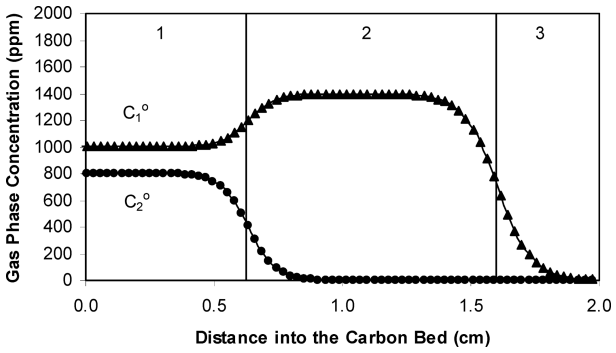

FIGURE 3. Wood-Snyder zones of vapor concentrations C_1^o and C_2^o within a 2-cm deep carbon bed challenged with a hypothetical mixture of two vapors. In most of Zone 1, the carbon is equilibrium saturated with both vapors. In most of Zone 2, Vapor 1 is at equilibrium at a higher (rollup) concentration than that entering the bed. In Zone 3, Vapor 1 is adsorbing from this higher concentration with the tail approaching breakthrough.

This reduces the problem to determining the equilibrium adsorbed capacities and gas phase concentrations of the vapor components in each zone. The IAST/DR/Bering equations (detailed below) provide the former.[11] Gas phase vapor concentrations in Zone 2 are increased by displacement of some of the vapors already adsorbed in Zone 2 by the OVs adsorbing in the expanding Zone 1 (in this example, mostly heptane). These vapor concentration increases (rollups) raise the capacities in Zone 2 and subsequent zones. Applying the principle of mass balance (total amounts of each vapor adsorbed in all the zones equals total amounts entering the

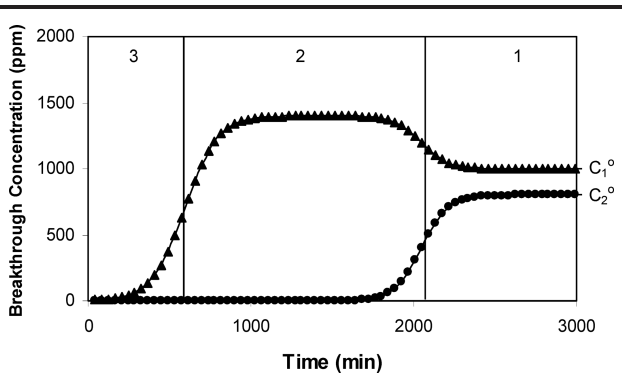

FIGURE 4. Wood-Snyder zones of vapor concentrations in bed effluent (breakthrough curves) for a hypothetical mixture of two vapors at concentrations C_1^o and C_2^o. Zones are defined as in Fig. 3.

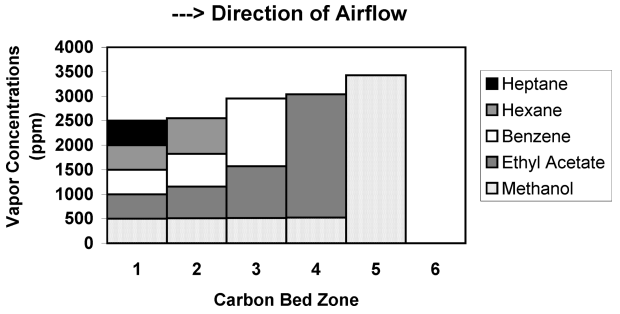

FIGURE 5. Vapor concentrations for the expanding bed equilibrium zone model for a hypothetical case of five vapors at 500 ppm each in the incoming air

bed) determines the rates of zone expansions and equilibrium breakthrough times.

OV Capacities and Distributions

The single vapor DR equation for n_i moles of vapor i with liquid molar volume V_{mi} (cm^3/mol) adsorbed in equilibrium with its vapor pressure p_i can be expressed as a modification of Eq. 2:

$$n_i(mol/g) = (W_o/V_{mi})\exp[-(RT/\beta_i E_o)^2\{\ln(p_{sati}/p_i)\}^2] \quad \textbf{(4)}$$

The Ideal Adsorption Solution Theory for mixtures of adsorbed vapors assumes equality of spreading pressures Π_i for each component. The DR-IAST equation for spreading pressure is:[11]

$$\Pi_i = \left(\frac{W_o\beta_i E_o\sqrt{\pi}}{2V_{mi}RT}\right)\left(1 - \text{erf}\left[\left(\frac{RT}{\beta_i E_o}\right)\ln\left(\frac{x_i\, p_{sati}}{p_i}\right)\right]\right) \quad \textbf{(5)}$$

where erf is the classical error function. In applying this model, spreading pressures for the components in each zone are balanced by adjusting the mole fractions, x_i, which must add up to unity. This gives adsorbed mixture component distributions in each zone but requires a second equation to determine total and component adsorbed capacities.

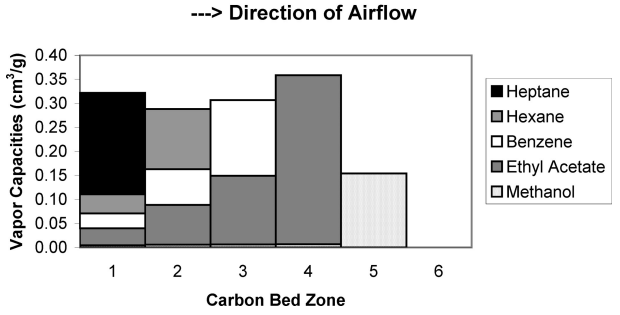

FIGURE 6. Adsorbed volumes for the expanding bed equilibrium zone model for a hypothetical case of five vapors at 500 ppm each in the incoming air

The Bering equation and Raoult's Law (Ideal Adsorbed Solution) provide total molar capacity, n_T, for each zone mixture by mole fraction weighting of affinity coefficient ($\beta_T = \Sigma x_i\beta_i$), partial liquid molar volume ($V_{mT} = \Sigma x_i V_{mi}$), and adsorption potential ($\varepsilon_T = \sum X_i\varepsilon_i = \Sigma x_i\, RT\ln[x_i p_{sati}/p_i]$) parameters of the components:[11]

$$n_T = \frac{W_o}{V_{mT}}\exp\left[-\left(\frac{RT}{E_o}\right)^2\left\{\frac{\Sigma x_i\ln(x_i p_{sati}/p_i)}{\beta_T}\right\}^2\right] \quad \textbf{(6)}$$

Component molar capacities are $n_i = x_i n_T$. Volume of adsorbed mixture is $V_{adsOV} = V_{mT}n_T$.

OV Rollups

Zone 1 is exposed to the entering OV concentrations; subsequent zones ($z > 1$) may be exposed to higher concentrations due to displacements of previously adsorbed vapors by more strongly adsorbed OVs. By mass balance the extent of concentration (g/cm^3) rollup depends on the airflow Q, the average speed of a zone movement W/τ_z (g/min), and the differences in volumetric adsorption capacities (cm^3/g) of OVs in adjacent Zones z and $z+1$:

$$\text{Rollup}C_{oi(z+1)} = C_{oi(z)} + \frac{(V_{adsOVi(z+1)} - V_{adsOVi(z)})(Wd_{Li})}{Q\tau_z} \quad \textbf{(7)}$$

where τ_z is the equilibrium breakthrough time of Zone z for carbon bed weight W and d_{Li} is liquid density of component i. Because of rollup effects, all the C_{oi} are replaced by $\text{Rollup}C_{oi}$ in each Zone $z > 1$ to calculate V_{adsOV} by the above equations. This is best accomplished by iterative computations.

Water Vapor Capacity

Water vapor is less efficiently adsorbed on carbon than OVs and much of it passes completely through the bed. All zones are exposed to any humidity that may be in the air and water may adsorb in each of them, reducing the micropore volumes available to the OVs. In the absence of OVs, the volume (cm^3/g carbon) of water adsorbed at equilibrium with relative humidity ($RH = p_{H2O}/p_{satH2O}$) air can be described by the DR equation:

$$V_{adsH2O} = W_o\exp\left\{-\left(\frac{R\,T}{\beta_{H2O}\,E_o}\right)^2(\ln(RH))^2\right\} \quad \textbf{(8)}$$

with the unitless water affinity coefficient β_{H2O}, a property of the carbon, in the range of 0.06.[2]

Because water adsorbs slowly on activated carbon, its equilibrium will be approached only with increasing time of exposure to humid air. The extent (fraction) of equilibrium reached at time t is:[2]

$$\text{Fract}_{H2O} = \left(1 - \exp\left[-\frac{0.00005(T - 273.15)v_L t}{d_B\sqrt{|\Delta A_{tot}|}}\right]\right) \quad \textbf{(9)}$$

where linear air flow velocity v_L is in cm/s, bed depth d_B is in cm, time t is in min, and ΔA_{tot} (g/g carbon) is the difference (+ or −) between two equilibrium water capacities.

The capacities at the exposure RH (Run RH) and at the RH (Pre RH) at which the carbon was previously equilibrated are obtained from applying the DR equation. For equilibrium or the same RH, this fraction is 1.00. Otherwise, it is applied to the difference in equilibrium water volumetric capacities, so that:

$$V_{adsH2O} = V_{ads}(\text{Pre RH}) + \text{Fract}_{H2O}[V_{ads}(\text{Run RH}) - V_{ads}(\text{Pre RH})] \quad \textbf{(10)}$$

Water Vapor Rollup

Zone 1 is exposed to the entering water vapor concentration; subsequent zones ($z > 1$) may be exposed to higher humidities from water rollup effects due to displacements of previously adsorbed water by OVs. The extent of RH rollup is calculated by an expression similar to Eq. 7 above:

$$\text{Rollup RH}_{(z+1)} = \text{RH}_{(z)} + \frac{(V_{adsH2O(z+1)} - V_{adsH2O(z)})(Wd_{H2O}RT)}{M_{wH2O}\, p_{satH2O}\, Q\tau} \quad \textbf{(11)}$$

where d_{H2O} is the density of water. The saturation vapor pressure of water p_{satH2O} at T has pressure units of atm for $R = 82.0254$ atm-cm^3/mol-deg. The upper limit of Rollup RH is 1.00. Because of water rollup effects, V_{ads}(Run RH) in Eq. 10 is replaced by $V_{ads}(\text{Rollup RH}_z)$ to calculate V_{adsH2O} as a function of time in each zone $z > 1$.

Alternately for initially dry beds, subsequent zones may be exposed to air drier than Run RH and heating due to water and OV adsorptions in Zone 1. These effects are not entirely taken into account by this model. They offset each other to some extent.

Effects of Water on Single OV Capacity

Having the parameters and equations to calculate the independent volumetric capacities of an OV and pure water, it becomes necessary to calculate capacities when both are adsorbed on activated carbon. The Volume Exclusion Theory provides:[2]

$$V_{adsOV} = (W_o - V_{adsH2O}) \exp\left\{ -\left(\frac{RT}{\beta_{OV}E_o}\right)^2 \left(\ln\frac{p_{satOV}}{p_{OV}}\right)^2 \right\} \quad \textbf{(12)}$$

$$V_{adsH2O} = (W_o - V_{adsOV}) \exp\left\{ -\left(\frac{R\,T}{\beta_{H2O}E_o}\right)^2 \left(\ln\frac{p_{satH2O}}{p_{H2O}}\right)^2 \right\} \quad \textbf{(13)}$$

for equilibrium volumes (cm^3/g) of the two adsorbates competing for available micropore volume W_o. Note that p_{H2O}/p_{satH2O} is relative humidity RH. These two linear equations can be solved analytically for the adsorbed volumes V_{adsH2O} and V_{adsOV}.

Water Solubility

One more contribution to V_{adsOV} needs to be included, that due to solubility, if any, of an OV in the adsorbed water phase, which is otherwise excluding the OV. The presence of condensed water enhances the capacity, improves retention, and extends breakthrough times of a water soluble OV, at least compared with what these would be if the OV were not water soluble. The OV adsorption potential in the presence of air at relative humidity RH is:[21]

$$\varepsilon_{RH} = \left(\frac{RTV_m}{\gamma_h - 0.28}\right)\left[\frac{1}{V_m}\ln\left(\frac{p_{sat}}{p}\right) - \frac{1}{18}\ln\left(\frac{1}{RH}\right)\right] \quad \textbf{(14)}$$

where $\gamma_h = 4.24\ (P_e/V_m)$ for OV molar volume V_m and molar polarizability P_e is the scale factor of an OV relative to heptane. For a completely water miscible OV in a water volume of V_{adsH2O} (calculated from Eqs. 8–13) the volume of OV adsorbed from the aqueous phase is:

$$V'_{adsOV} = V_{adsH2O} \exp[-(\varepsilon_{RH}/\beta_{OV}E_o)^2] \quad \textbf{(15)}$$

For a less soluble OV this is multiplied by a solubility factor S_f defined as the fraction in parts by liquid volume of OV that can be dissolved in one part of water volume. The range of S_f is taken to be from zero for a totally immiscible OV to 1.0 for a totally miscible one. A conservative estimate for S_f is zero, but this should not be used for alcohols, amines, or other polar compounds, which are often to some extent water-soluble.

The total gravimetric capacity (g/g carbon) of the activated carbon for the OV in the presence of adsorbed water then becomes:

$$W_{e,OVtotal} = (V_{adsOV} + V'_{adsOV})d_L \quad \textbf{(16)}$$

Effects of Water on OV Mixture Capacity

A significant new assumption of this multivapor, all-humidity model is that an adsorbed OV mixture in each zone behaves as a single pseudo-liquid with properties (adsorption potential, liquid density, molecular weight, etc.) weighted according to the mole fractions of components in the mixture. Water is then in competition with this pseudo-liquid for micropore volume according to the above equations. On the other hand, solubilities of mixture components in adsorbed water, which may add to capacities in each zone, are handled separately for each vapor.

OV Adsorption Rates

Once equilibrium capacities for each vapor in each zone are established, finite adsorption rates are added to change the flat wave fronts to the observed reversed and stretched "S" shapes (e.g., Figure 3). These are described by Eq. 1, where breakthrough times are reduced from the equilibrium values (first term) by incorporating the kinetics in the second term.

Rate coefficients k_v for each vapor wavefront are calculated using the Wood-Lodewyckx correlation for $C/C_o = 0.1\%$ breakthrough fraction:[22]

$$k_{v0.1\%} = 800\beta_{OV}^{0.33}v_L^{0.75}d_p^{-1.5}(W_e/M_w)^{0.5}\ \text{min}^{-1} \quad \textbf{(17)}$$

where linear flow velocity v_L (cm/s) $= Q/60A_B$ for bed cross section area A_B (cm^2); d_p (cm) = average carbon granule diameter; M_w (g/mol) = molecular weight of the OV; and $\beta_{OV} = 0.0862P_e^{0.75}$.[23]

Skew corrections are used to calculate rate coefficients at other breakthrough fractions (up to $C/C_o = 0.5$) as:[24]

$$k_{v(C/Co)} = \left[\frac{1 + b\ln(C_o/C - 1)}{1 + b\ln(999)}\right] k_{v0.1\%} \quad \textbf{(18)}$$

where b is a quadratic root solution of a correlation for the skew parameter $S = k_{v1\%}/k_{v10\%}$:

$$S = 1.41 - 0.0000324\left[\frac{1 + b\ln(9)}{1 + b\ln(C_o/C - 1)}\right] k_{v(C/Co)} \quad \textbf{(19)}$$

which has a lower limit $S \geq 1$.

Next, rate coefficient correction factors reported by Wood for orders of elution are applied to the resulting $k_{v(C/Co)}$: 1.00 for first eluting, 0.85 for second, and 0.56 for subsequent.[14]

Because adsorbed water has an effect on OV adsorption rates the OV adsorption rate coefficient is further corrected by:[25]

$$k^{Wet}_{v(C/Co)} = \left[0.3 + 0.7\left(\frac{W^{Wet}_e}{W^{Dry}_e}\right)\right] k^{Dry}_{v(C/Co)} \quad \textbf{(20)}$$

This has an upper limit of k^{Dry}_v.

Model Application

Because there are many interacting effects between the OVs and water vapor, application of this model, such as in a spreadsheet or computer program, requires iterations to attain a final answer. First, water presence and vapor rollups are ignored. During repeated iterations, OV rollup in each zone is calculated, increasing vapor concentrations and adsorbed concentrations. After iterations produce fixed OV capacities in each zone, water vapor is introduced and its effects calculated. Further iterations with water vapor included are repeated until fixed capacities and breakthrough times result. The input parameters required are the same as with the single vapor model and program: (1) cartridge and carbon parameters, (2) organic vapors and water parameters, and (3) use condition parameters. See input parameter descriptions with Eqs. 1 and 2 above.

Experimental

The 3M cartridge used in this work (#7251; 3M St. Paul, Minn.) has a cylindrical geometry for which it was easy to construct a gastight holder (described below) for testing. Cartridges were used as received, one at a time. Carbon bed dimensions were reported by the manufacturer to be 7.6 cm diameter and 2.25 cm deep for 44.5 g of adsorbent. These are also the parameters used in the model, along with a calculated packed density of 0.436 g/cm^3. The carbon granules were reported by the manufacturer to be 12–16 mesh, so an average diameter of 0.14 cm was used in the model. Chemicals used were ACS certified reagents or better.

The experimental apparatus is diagrammed in Figure 7. A Miller/Nelson Flow-Temperature-Humidity Control System (model HCS-401; Miller-Nelson Research, Inc., Monterey, Calif.) was used to generate a constant air source of known temperature and relative humidity. Compressed air filtered for organics and particulates fed the Miller/Nelson unit. Water used by the Miller/Nelson unit was tap water that was run

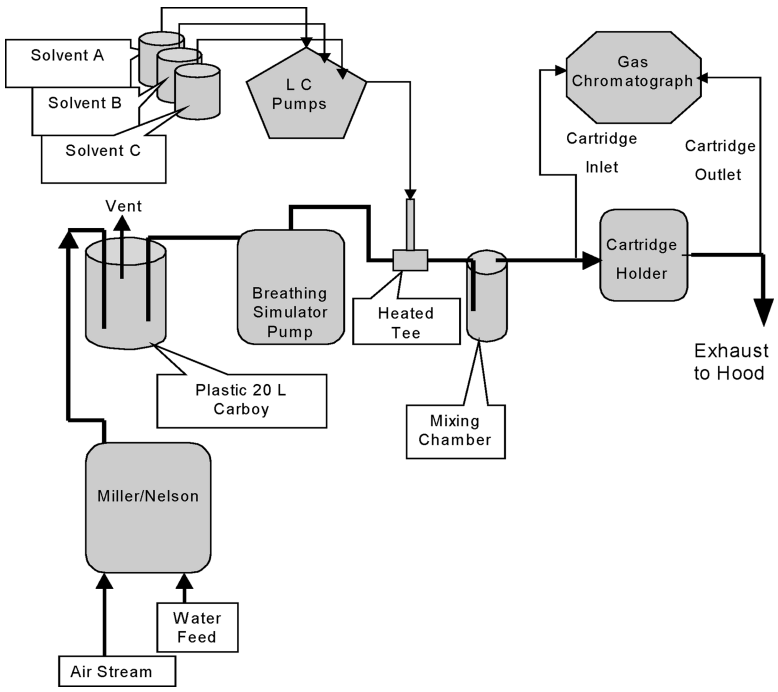

FIGURE 7. Experimental setup

through a deionizing cartridge prior to use. The output from the Miller/Nelson was vented into a large plastic carboy with a volume of approximately 20 liters. This was used as a reservoir from which conditioned air could be drawn. The input was maintained at a substantially greater rate (60 L/min) than output so that dilution with outside air did not occur.

The intake of a breathing simulator pump (model SH55E, Scott Aviation Corporation, Lancaster, N.Y.) was inserted into the carboy to extract 33 to 37 L/min of conditioned air at 25 cycles per min. The breathing pump was used with a cam to simulate the pulsed effect that occurs during the human breathing cycle. The exhalation cycle flow was vented to the atmosphere to simulate respirator operation with an exhalation valve and a backflow valve to prevent reverse flow through the cartridge. The effluent stream from the pump was ultimately connected to the cartridge holder.

Before that connection, a tee was placed in the air line so that liquids could be introduced to produce vapor in the airstream. The tee was wrapped with heating tape to slightly elevate the temperature so the liquid contaminants would flash evaporate on entering the gas stream. There was sufficient distance from the tee to the cartridge to allow cooling to ambient temperature. Liquid chromatographic (LC) pumps (model 210, SRI Instruments, Inc., Torrance, Calif.) were used to dispense the liquid chemicals. The effluent streams of the pumps were connected in parallel so that varying amounts of liquids could be independently controlled to yield various concentrations of vapors in the gas stream. For the results reported here, one or three pumps were used at a time. After the vapor was introduced, the airstream passed through a sealed 5-L container to provide mixing for uniform concentrations.

The vapor(s) in the airstream from the mixing container then passed into an aluminum housing that held the cartridge to be tested. This housing was a two-piece system clamped together with an o-ring around the cartridge to provide a leak-proof fit. The incoming gas stream to the cartridge holder was tapped with a $^1/_8$-inch Teflon tube connected to a gas chromatograph. A similar connection was made to the stream exiting the holder. This provided a means to monitor the vapor concentrations entering and exiting the cartridge being tested.

The vapor monitor consisted of an SRI model 8610 dual-column, dual-flame detector, gas chromatograph (GC) also manufactured by SRI, Inc. It was equipped with two 10-port automated values with 1 mL sample loops. It used PeakSimple software provided by SRI, Inc. The GC could be programmed to automatically sample the two (cartridge input and output) gas streams, quantify the concentrations, and store the values in an Excel spreadsheet for future use. The columns, RTX-5, 30 m long × 0.053 mm ID and 1.0-micron film thickness (Restek, Bellefonte, Pa.) were operated at 120°C and 5-mL/min hydrogen carrier flows. All components could be separated in under 3 min. This permitted simultaneous monitoring of the input and exhaust of the cartridge at 3-min intervals.

The GC responses for each chemical vapor were calibrated by using standards produced in the laboratory as follows. A 10-L gas bag was filled with 6 L of air. An appropriate amount of solvent was injected using a microliter liquid syringe. The vapor and air were mixed by kneading the gas bag. A sample of the standard was injected into the gas sampling loop of the gas sampling valve. Thus, the same plumbing was used for calibration and analysis of unknowns. This was done at a frequency of once or twice a day depending on the length of analysis time. In all cases, the GC was found to hold calibration very well. The lower detection limits for these organic vapors were on the order of 1 ppm, as determined by the first detectable peaks above baseline noise.

Airflows into the cartridge were calibrated by using a model DTM-325 dry gas meter (American Meter Company, Horsham, Pa.). Ambient temperature and atmospheric pressure were recorded. Ambient temperature was steady enough and RH was low enough ($\leq$85%) to avoid condensation in air lines.

The LC pump(s) and breathing pump were operated until a steady-state condition existed, typically 1 to 2 hours, so that consistent concentrations could be generated before introducing the test cartridge. Once the concentration(s) reached steady state, the solvents in the LC pump reservoirs were weighed. While a reservoir was being weighed, its LC pump was switched to an alternate reservoir of the same liquid to avoid upsetting the steady-state generation of vapors. Knowing the weight of solvent used and the concentration going into and out of the cartridge, a mass balance could be done as a check on calibrations. The cartridge was then quickly inserted into the aluminum holder so that vapors in the airstream could be forced through it. The test and GC software were started at this time. Data collection by the GC was usually continued until the breakthrough curve of the third component of each mixture was completed.

Model Testing with Literature Data

The first set of data examined to test the service life estimation model for mixtures was the extensive data of Yoon and Lara et al.[16–19] at dry conditions. These are discussed in the Background section. They observed full breakthrough curves of single vapors and OV mixtures for single cartridges at 24 L/min airflow, 25°C, and 40% RH. The cartridges were as-received Scott Aviation Model 642-OV containing 50 g (112 cm^3) of 12–20 mesh coconut-based activated carbon. They fit breakthrough curve data as ln[P/(1-P)] vs. time t to a linear form of the Reaction Kinetic equation:

$$t = \tau + \frac{1}{k'} \ln\left(\frac{P}{1-P}\right) \qquad \textbf{(21)}$$

where in terms used in Eq. 1, $P = C/C_o$. Results were reported as τ and k'. According to Eq. 1, $\tau = W_e\, W/C_o\, Q$ and $k' = k_v C_o/W_e \rho_B$.

Lara et al.[19] supplemented these data with data for toluene/m-xylene mixtures at 36 L/min through pairs of the same cartridges. However, they reported the results as total volumetric capacities W_v (cm^3/cartridge) $= W_e W/d_L$, as

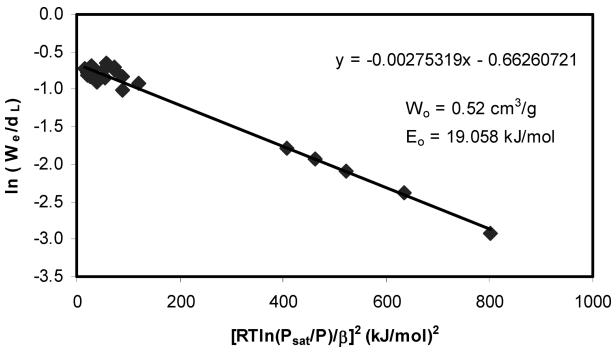

FIGURE 8. Dubinin-Radushkevich plot for Yoon, Lara et al.[16–19] single vapor data for acetone, m-xylene, styrene, and toluene.

$C/C_o = 0.5$ breakthrough times τ, and as 10% breakthrough times $t_{10\%}$.

Comparisons with model estimations required experimental 10% breakthrough times $t_{10\%}$ for the Yoon data as well, and so these were calculated from reported τ and k' using Eq. 21 with $P = 0.10$.

For application of the new model, the micropore volume W_o and adsorption potential E_o parameters were required for the carbon used in the Scott cartridges. These were obtained from a DR plot (Figure 8). Equation 1 was used to derive W_e/d_L (cm^3/g carbon) from τ C_oQ/Wd_{Li}, which is obtained from reported τ for single vapor measurements. Then from Eq. 2 a plot of $\ln(W_e/d_L)$ versus $[(RT/\beta)\ln(P_{sat}/P)]^2$ gave the slope and intercept, which led to $W_o = 0.52$ cm^3/g and $E_o = 19.058$ kJ/mol.[2]

Putting these and other cartridge, vapor, and use conditions parameters into the model yielded 10% breakthrough times. These results are compared with experimental ones in Figure 9. The data are identified by orders of elution from the cartridges determined by model values of τ. The line on the graph is the equivalence line. Standard deviation (SD) of estimates from experimental values was 27 min (relative standard deviation RSD = 8%) for 66 first and second eluting vapors with an average bias = +1.6% and a correlation coefficient of R = 0.997. Relative standard deviation of estimates for seven third and fourth eluting vapors was 34%, largely due to an average bias of −14%. There is no satisfactory explanation for this latter bias, but it is conservative for setting change-out schedules using the model. For all 73 data sets SD = 32 min, RSD = 9%, Bias = +0.1%, and R = 0.988.

The second set of literature data used for model testing was that of Swearengen and Weaver.[26,27] They reported average (of 6) 1% and 10% breakthrough times of methyl ethyl ketone (MEK), isopropyl alcohol (IPA), hexane, butyl acetate, and ethyl benzene alone and in binary mixtures at low (20% or 50% RH) and high (85% RH) humidities. The MSA respirator cartridges containing 12-20 mesh petroleum-based activated carbon were used at 40 L/min airflow in pairs, as received or for one MEK/IPA mixture with cartridges equilibrated at the test humidities.[27]

For the previous single-vapor, all-humidity model, data from these authors for dry, single-vapor experiments were used to make a DR plot and obtain micropore volume $W_o = 0.606$ cm^3/g and adsorption potential $E_o = 18.70$ kJ/mol.[2] Also, $W_o = 0.506$ cm^3/g (not the typographical error 0.560) was assumed for the denser carbon (presumably used at the AR/85% RH condition) and $\beta_{H2O} = 0.06$ for the water affinity coefficient. These same parameters have been used for the following binary mixture estimates and comparisons.

Figures 10 and 11 show comparisons of model-calculated single vapor and mixture components' 1% breakthrough times with experimental ones at dry and high humidity conditions, respectively. Differences (n = 16 each) from the experimental values for the dry and humid mixtures yielded (SD = 11 min, RSD = 15%, Bias = +17%, and R = 0.944) and (SD = 15 min, RSD = 32%, Bias = +13%, and R = 0.867), respectively.

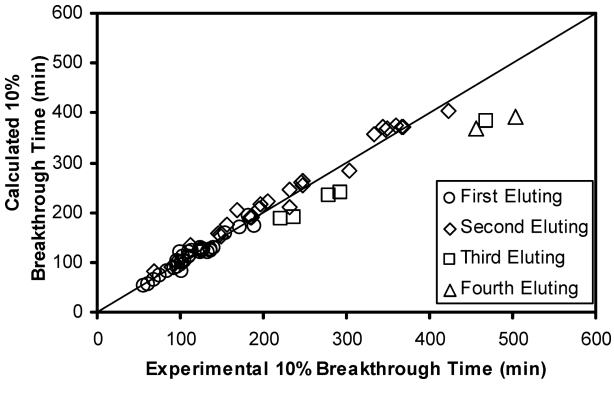

FIGURE 9. Model-calculated 10% breakthrough times vs. experimental ones for all binary, ternary, and quaternary mixtures from the work of Yoon, Lara et al.[16–19] The line is the equivalence line.

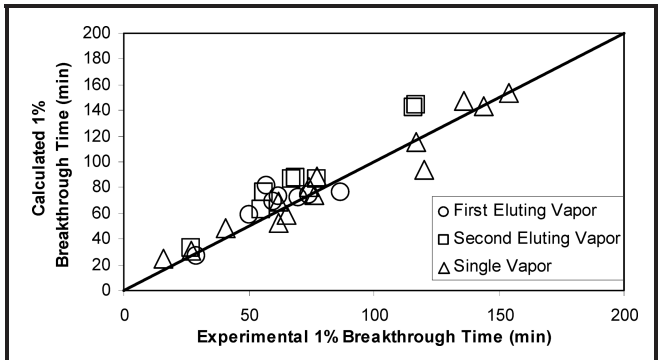

FIGURE 10. Comparisons of model-calculated single vapor and mixture components' 1% breakthrough times with experimental ones at dry conditions from the work of Swearengen and Weaver[26,27]

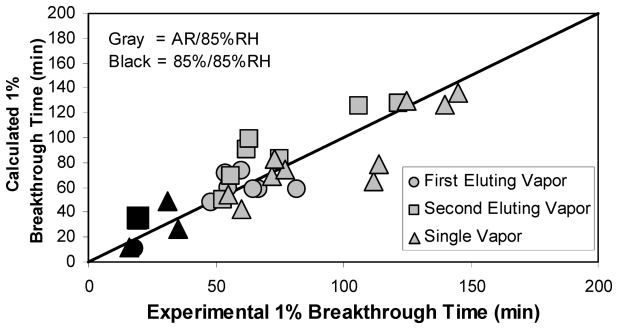

FIGURE 11. Comparisons of model-calculated single vapor and mixture components' 1% breakthrough times with experimental ones at high humidity conditions from the work of Swearengen and Weaver[26,27]

The third set of literature data analyzed was that of Cohen et al.[28] with binary mixtures of carbon tetrachloride and hexane or pyridine at 50% RH. They reported 10% breakthrough times corrected to 1000 ppm for both MSA cartridges and respirator cartridge tubes. For model calculations for mixtures, the carbon parameters $W_o = 0.75$ cm^3/g and $E_o = 14.78$ kJ/mol developed previously were used.[2] Figure 12 shows the comparison of model-calculated 10% breakthrough times with experimental ones. The differences of estimates from experimental values ($n = 18$) yielded SD = 20 min, RSD = 21%, Bias = −0.5% and $R = 0.970$.

Model Testing with New Data

Experimental studies were done with two ternary mixtures to supplement the existing data and to test the multivapor model at high humidities. Figures 13 and 14 show examples of raw data breakthrough curves with measurements at 3-min intervals. In the first case (Experiment 12 in Table I), the mixture consisted of approximately 360 ppm each of acetone, trichloroethylene, and m-xylene at 80% RH and about 36 L/min cyclic airflow. The gap at about 67–81 min was due to a brief pause in the experiment to refill the LC pumps' supplies.

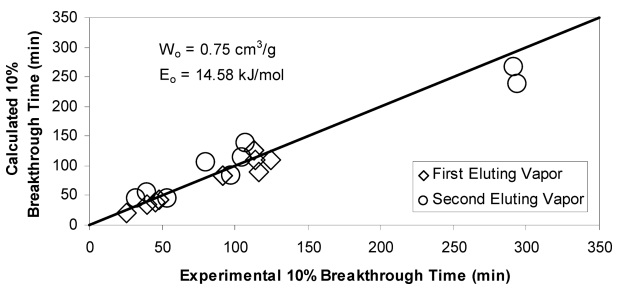

FIGURE 12. Calculated breakthrough times vs. experimental ones for respirator cartridges and respirator cartridge tubes for dry mixtures of carbon tetrachloride and hexane or pyridine from Cohen et al.[28]

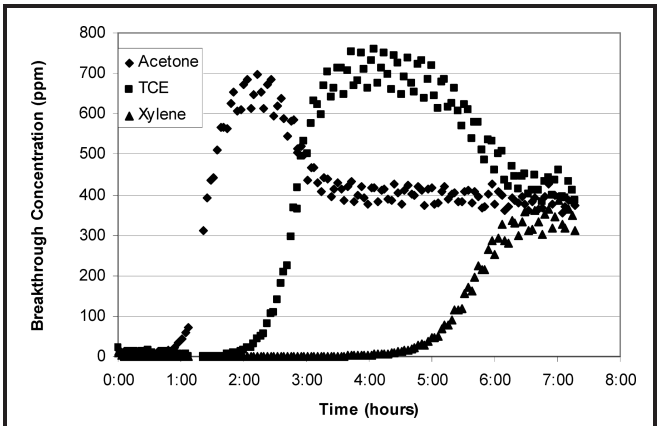

FIGURE 13. Raw data plot of breakthrough curves for a mixture of about 350 ppm each of acetone, trichloroethylene, and m-xylene at 80% RH (Experiment 12)

Data scatter increased as the cartridge approached saturation in each vapor. At these points, breakthrough concentrations become very sensitive to slight variations in concentrations and cycling flow rate of the incoming vapors. This scatter demonstrates the responsiveness of the gas chromatographic analysis. At the important regions, less than 50% breakthrough, the breakthrough curves are smooth, which permits breakthrough times to be obtained reliably.

Figure 14 is for Experiment 17 (Table I) with approximately 280 ppm each of cyclohexane, methyl isobutyl ketone (MIBK), and toluene at 75% RH and about 36 L/min. Unlike in Figure 13 the latter two vapors were co-eluting but at differing rates. Striking features of these graphs are the rollups of the first and second eluting vapors, where breakthrough concentrations temporarily exceeded the incoming concentrations until the cartridge was completely saturated with all three vapors.

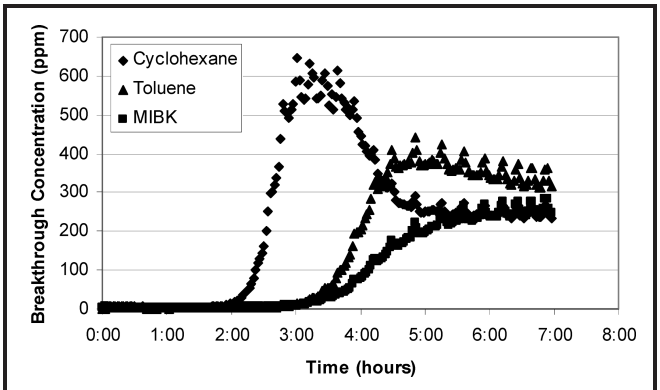

FIGURE 14. Raw data plot of breakthrough curves for a mixture of about 300 ppm each of cyclohexane, toluene, and methyl isobutyl ketone at 75% RH (Experiment 17)

TABLE I. Experimental and Model Near 10% Breakthrough Times with Experimental Parameters for Ternary Mixtures at High Humidities

Exp #	Vapor Observed	t_b Meas (min)	t_b Calc (min)	Breakthrough Fraction C/C_o	Avg. Conc. $\langle C_o \rangle$ (ppm)	Covapor 1	Avg. Conc. $\langle C_o \rangle$ (ppm)	Covapor 2	Avg. Conc. $\langle C_o \rangle$ (ppm)	T (°C)	P (atm)	RH %	Flow Rate Q (L/min)
8	Acetone	86.3	45.6	0.092	221.1	TCE	196.6	m-Xylene	170.9	25	0.97	45	36.2
8	TCE	281.7	266.8	0.095	198.9	Acetone	190.2	m-Xylene	176.4	25	0.97	45	36.2
8	m-Xylene	676.4	638.1	0.110	177.6	Acetone	180.0	TCE	199.1	25	0.97	45	36.2
11	Acetone	64.6	35.9	0.093	325.3	TCE	362.1	m-Xylene	346.6	24	0.97	66	36.2
11	TCE	152.1	173.3	0.114	361.5	Acetone	315.5	m-Xylene	347.4	24	0.97	66	36.2
11	m-Xylene	Experiment interrupted before breakthrough											
12	Acetone	61.0	35.5	0.126	356.0	TCE	377.0	m-Xylene	357.7	24	0.97	80	36.2
12	TCE	133.1	151.7	0.119	361.1	Acetone	372.2	m-Xylene	351.1	24	0.97	80	36.2
12	m-Xylene	296.4	329.7	0.106	357.3	Acetone	391.2	TCE	382.5	24	0.97	80	36.2
13	Acetone	45.0	14.9	0.101	623.0	TCE	591.1	m-Xylene	501.7	23	0.97	85	36.2
13	TCE	92.6	94.1	0.096	597.6	Acetone	611.9	m-Xylene	534.6	23	0.97	85	36.2
13	m-Xylene	210.2	218.2	0.095	532.2	Acetone	605.9	TCE	596.2	23	0.97	85	36.2
47	Acetone	55.8	31.9	0.110	505.4	TCE	500.8	m-Xylene	522.3	24	0.97	81	37.2
47	TCE	117.8	107.0	0.077	502.8	Acetone	532.0	m-Xylene	514.8	24	0.97	81	37.2
47	m-Xylene	310.1	247.8	0.171	513.8	Acetone	577.6	TCE	506.0	24	0.97	81	37.2
48	Acetone	49.6	30.5	0.059	536.9	TCE	513.1	m-Xylene	531.1	25	0.97	81	33.7
48	TCE	96.1	125.9	0.195	512.5	Acetone	532.8	m-Xylene	533.8	25	0.97	81	33.7
48	m-Xylene	254.3	243.4	0.096	536.5	Acetone	527.1	TCE	515.0	25	0.97	81	33.7
24	Cyclohexane	61.3	61.0	0.086	566.0	MIBK	572.0	Toluene	562.6	24	0.97	89	36.2
24	MIBK	98.8	92.3	0.091	574.3	Cyclohexane	569.8	Toluene	566.4	24	0.97	89	36.2
24	Toluene	98.8	109.1	0.118	566.4	Cyclohexane	569.8	MIBK	574.3	24	0.97	89	36.2
35	Cyclohexane	35.6	42.4	0.090	1193.0	MIBK	1132.1	Toluene	921.3	26	0.97	80	35.5
35	MIBK	53.9	63.9	0.083	1143.9	Cyclohexane	1175.3	Toluene	919.2	26	0.97	80	35.5
35	Toluene	56.9	77.1	0.099	918.6	Cyclohexane	1174.5	MIBK	1143.1	26	0.97	80	35.5
68	Cyclohexane	49.6	44.9	0.130	924.9	MIBK	958.0	Toluene	946.8	24	0.96	89	37.0
68	MIBK	80.6	64.2	0.101	975.5	Cyclohexane	940.6	Toluene	968.4	24	0.96	89	37.0
68	Toluene	80.6	75.2	0.102	968.4	Cyclohexane	940.6	MIBK	975.5	24	0.96	89	37.0
17	Cyclohexane	129.0	123.1	0.089	270.6	MIBK	285.2	Toluene	301.8	23	0.97	75	36.2
17	MIBK	216.8	194.3	0.104	286.7	Cyclohexane	273.7	Toluene	308.0	23	0.97	75	36.2
17	Toluene	203.1	216.7	0.108	307.9	Cyclohexane	273.7	MIBK	286.9	23	0.97	75	36.2
23	Cyclohexane	63.1	74.4	0.112	510.8	MIBK	534.0	Toluene	526.2	23	0.97	82	36.2
23	MIBK	103.9	109.6	0.109	557.0	Cyclohexane	543.5	Toluene	544.0	23	0.97	82	36.2
23	Toluene	98.8	126.8	0.112	542.9	Cyclohexane	541.0	MIBK	556.0	23	0.97	82	36.2

Note: TCE = trichloroethylene; MIBK = methyl isobutyl ketone.

Breakthrough curves and times with single vapors were measured to establish carbon parameters.[2] Figure 15 shows the DR plot from 26 measurements with six different vapors at dry conditions. Sampling times nearest midpoints of the breakthrough curves were interpolated to calculate the equilibrium times τ and capacities W_e. Cumulative averages (trapezoidal time integration from exposure starting times) of concentrations measured at 3-min intervals were used for partial pressures p_i. The tight scatter around a straight line confirms the quality of the experiments. The linear least-squares, best-fit line shown on the graph yielded slope and intercept corresponding to adsorption potential $E_o = 15.863$ kJ/mol and micropore volume $W_o = 0.783$ cm^3/g, respectively. From thirteen high humidity (75–91% RH) single-vapor experiments with four low-solubility vapors, an average water affinity coefficient of $\beta = 0.06$ was obtained with a standard deviation of 0.02.

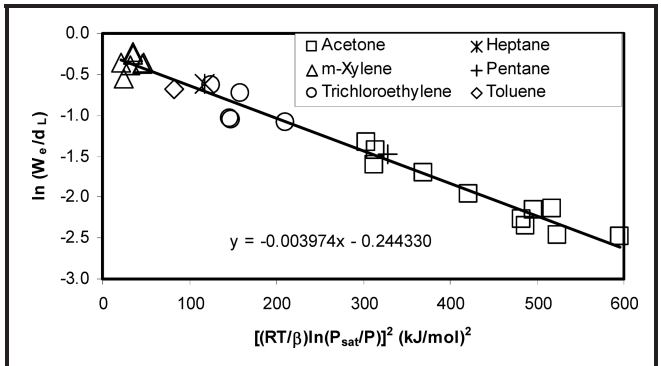

FIGURE 15. Dubinin-Radushkevich plot for the 3M 7251 cartridge obtained by breakthrough studies with six single vapors at dry conditions

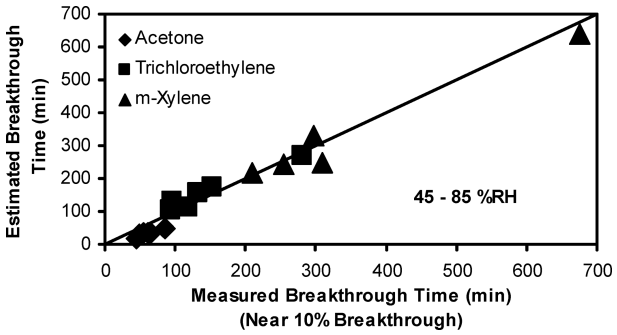

FIGURE 16. Model-calculated breakthrough times vs. experimental ones for ternary mixtures of acetone, trichloroethylene, and m-xylene at high humidities

Using these carbon parameters with cartridge parameters, vapor parameters, and test conditions, breakthrough times for mixture components were calculated using the model described above. Experimental challenge concentrations measured for each vapor at 3-min intervals were integrated using trapezoidal approximation from zero time to get cumulative concentrations. Measured breakthrough concentrations nearest 10% of these cumulative concentrations were used to get C/C_o values for use in the calculations. Breakthroughs of 10% were assumed for covapors; this fraction is arbitrary, but necessary for the model calculations.

Figures 16 and 17 and Table I show 32 comparisons of the model-calculated breakthrough times versus measured times (nearest 10% breakthrough) for the two ternary vapor combinations at the humidities shown in Table I over the range of 45–89% RH. Methyl isobutyl ketone and toluene often co-eluted with overlapping breakthrough curves (e.g., Figure 14). Graphed points clustering around the equivalence lines show good agreements with SD = 22 min, RSD = 25%, Bias = −5%, and R = 0.984. Acetone estimates were generally low (conservative), possibly due to its high water solubility (completely miscible), which may not be sufficiently accounted for by the model, and/or possibly due to reactivity with water (hydrolysis, perhaps catalyzed by the carbon). Excluding acetone, the differences of estimates from 26 measurements of the other five vapors at 45–89% RH yielded SD = 21 min, RSD = 15%, Bias = +4%, and R = 0.989.

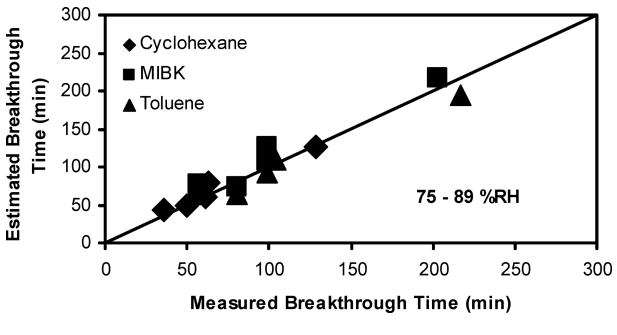

FIGURE 17. Model-calculated breakthrough times vs. experimental ones for ternary mixtures of cyclohexane, methyl isobutyl ketone, and toluene at high humidities

CONCLUSIONS

The good agreements of model predictions with experimental breakthrough times at dry conditions (Figures 9, 10, 12) and at humid conditions (Figures 11, 16, 17) demonstrate that the model gives reasonably good estimates for establishing service lives. Breakthrough times of all components of the mixtures (except acetone at high humidities, as explained above) were successfully predicted at all humidity levels. This included co-eluting vapors. Both experimental and model errors contribute to any differences.

As in the previous single-vapor models, the carbon parameters (micropore volume, adsorption potential, and water affinity coefficient) must be known or established from single-vapor experimental data. Ideally, they would be available from carbon and respirator cartridge manufacturers, along with cartridge parameters (carbon bed depth, diameter, effective granule size and number of cartridges on a respirator).

For the model calculations and comparisons presented in this article, the multivapor model has been implemented as a spreadsheet (initially) and as a Microsoft Visual Basic program. Both required iterations of rollups of vapor concentrations and relative humidities to converge to breakthrough time results. This is very tedious in a spreadsheet and was used in this paper only for dry conditions. However, with the computer program, the iterations were handled automatically and answers obtained quickly for both humid and dry conditions.

Properly implemented, this multivapor model can give results for one vapor as well as for more. Therefore, it can be a replacement, as well as an extension, of the single-vapor, all-humidity model and program.[2,8] Gases, which are removed by reaction instead of by micropore condensation, must be handled differently.[3]

REFERENCES

1. "Respiratory Protection; Final Rule," *Federal Register 63*:5 (8 January 1998). pp. 1152–1300.
2. **Wood, G.O.:** Estimating service lives of organic vapor cartridges II: A single vapor at all humidities. *J. Occup. Environ. Hyg. 1*:472–492 (2004).
3. **Wood, G.O.:** Estimating service lives of air-purifying respirator cartridges for reactive gas removal. *J. Occup. Environ. Hyg. 2*:414–423 (2005).
4. **U.S. Department of Labor (USDOL), Occupational Safety and Health Administration (OSHA):** *Inspection Procedures for the Respiratory Protection Standard*. OSHA Instruction, Directive Number CPL 02-00-120, Effective date September 25, 1998. Standard Number 1910.134. http://www.osha.gov/pls/oshaweb/owadisp.show_document?p_table=DIRECTIVES&p_id=2275.
5. "Factors That Can Reduce Cartridge Service Life." [Online] Available at http://www.osha.gov/SLTC/etools/respiratory/factors/factors.html.

6. **Wood, G.O.:** Estimating service lives of organic vapor cartridges. *Am. Ind. Hyg. Assoc. J. 55*:11–15 (1994).
7. **Wheeler, A.:** *Catalysis*. Volume II, P.H. Emmett (ed.). New York: Reinhold, 1955. p. 105.
8. **Department of Labor, Occupational Safety and Health Administration:** "Breakthrough: Single Vapor, Version 3.0.2." Available at www.osha.gov/SLTC/etools/respiratory/advisor_genius_wood/breakthrough.html.
9. **Dubinin, M.M., E.D. Zaverina, and L.V. Radushkevich:** Sorption and structure of active carbons. I. Adsorption of organic vapors. *Zh. Fiz. Khim. 21*:1351–1362 (1947).
10. **Wood, G.O.:** "Reviews of Models for Adsorption of Single Vapors, Mixtures of Vapors, and Vapors at High Humidities on Activated Carbon for Applications Including Predicting Service Lives of Organic Vapor Respirator Cartridges" (Report LA-UR-00-1531). Los Alamos, N.M.: Los Alamos National Laboratory, 2000.
11. **Wood, G.O:** Review and comparisons of D/R models of equilibrium adsorption of binary mixtures of organic vapors on activated carbons. *Carbon 40*:231–239 (2002).
12. **Grant, R.J., and M. Manes:** Adsorption of binary hydrocarbon gas mixtures on activated carbon. *Ind. Eng. Chem. Fundam. 5*:490–498 (1966).
13. **Myers, A.L., and J.M. Prausnitz:** Thermodynamics of mixed-gas adsorption. *AIChE J. 11*:121–127 (1965).
14. **Wood, G.O.:** A review of the effects of covapors on adsorption rate coefficients of organic vapors adsorbed onto activated carbon from flowing gases. *Carbon 40*:685–694 (2002).
15. **Cooney, D.O., and F. P. Strusi:** Analytical description of fixed-bed sorption of two Langmuir solutes under nonequilibrium conditions. *Ind. Eng. Chem. Fundam. 11*:123–126 (1972).
16. **Yoon, Y.H., J.H. Nelson, J. Lara, C. Kamel, and D. Fregeau:** A theoretical interpretation of the service life of respirator cartridges for the binary acetone/m-xylene system. *Am. Ind. Hyg. Assoc. J. 52*:65–74 (1991).
17. **Yoon, Y. H., J. H. Nelson, J. Lara, C. Kamel, and D. Fregeau:** A theoretical model for respirator cartridge service life for binary systems: Application to acetone/styrene mixtures. *Am. Ind. Hyg. Assoc. J. 53*(8):493–502 (1992).
18. **Yoon, Y.H., J.H. Nelson, and J. Lara:** Respirator cartridge service-life: Exposure to mixtures. *Am. Ind. Hyg. Assoc. J. 57*:809–819 (1996).
19. **Lara, J., Y.H. Yoon, and J.H. Nelson:** The service life of respirator cartridges with binary mixtures of organic vapors. *J. Int. Soc. Resp. Prot. 1995(Spring)*:7–26 (1995).
20. **Vahdat, N.:** Theoretical study of the performance of activated carbon in the presence of binary vapor mixtures. *Carbon 35*:1545–1557 (1997).
21. **Wohleber, D.A., and M. Manes:** Application of the Polanyi adsorption theory to adsorption from solution on activated carbon. III. Adsorption of miscible organic liquids from water solution. *J. Phys. Chem. 75*:3720–3723 (1971).
22. **Wood, G.O., and P. Lodewyckx:** An extended equation for rate coefficients for adsorption of organic vapors and gases on activated carbons in air-purifying respirator cartridges. *Am. Ind. Hyg. Assoc. J. 64*:646–650 (2003).
23. **Wood, G.O.:** Affinity coefficients of the Polanyi/Dubinin adsorption isotherm equations. A review with compilations and correlations. *Carbon 39*:343–356 (2001).
24. **Wood, G.O.:** Quantification and application of skew of breakthrough curves for gases and vapors eluting from activated carbon beds. *Carbon 40*:1883–1890 (2002).
25. **Wood, G.O., and P. Lodewyckx:** Correlations for high humidity corrections of rate coefficient for adsorption of organic vapors and gases on activated carbons in air-purifying respirator cartridges. *J. Int. Soc. Resp. Prot. 2002(Spring/Summer)*:58–64.
26. **Swearengen, P.M., and S.C. Weaver:** Respirator cartridge study using organic-vapor mixtures. *Am. Ind. Hyg. Assoc. J. 49*:70–74 (1988**).**
27. **Swearengen, P.M., and S.C. Weaver:** The effect of organic vapor mixtures on the service life of respirator cartridges. In *Proceedings of the 1985 Scientific Conference on Chemical Defense Research* (Report CRDC-SP-86007), M. Rausa (ed.). Aberdeen Proving Ground, Md.: U.S. Army Chemical Research and Development Center, April 1986. pp. 941–949.
28. **Cohen, H.J., D.E. Briggs, and R.P. Garrison:** Development of a field method for evaluating the service lives of organic vapor cartridges—Part III: Results of laboratory testing using binary organic vapor mixtures. *Am. Ind. Hyg. Assoc. J. 52*:34–43 (1991).